Carbon-addition-induced bulk ZrTiCuNiBe amorphous matrix composite containing ZrC particles

Wei Hua Wang [a,*], Hai Yang Bai [b]

[a] *Institute of Physics, Chinese Academy of Sciences, Beijing 100080, People's Republic of China*
[b] *Cryogenic Laboratory, Chinese Academy of Sciences, Beijing 100080, People's Republic of China*

Abstract

Bulk $Zr_{41}Ti_{14}Cu_{12.5}Ni_{10}Be_{22.5}$ amorphous matrix composites (AMCs) were synthesized by solid–liquid phase reaction between added carbon and constituents of the molten Zr–Ti–Cu–Ni–Be glass-forming alloy. The structure, thermal and mechanical properties were investigated by means of X-ray diffraction (XRD), differential scanning calorimetrically and microhardness measurements. It was found that the reaction-induced crystalline ZrC particles are uniformly distributed in the amorphous matrix. The thermal properties and glass-forming ability (GFA) of the amorphous matrix are not significantly changed up to 4% carbon addition, while the strength of the composite is significantly improved. The strengthening mechanism in the bulk AMC is discussed. © 2000 Elsevier Science B.V. All rights reserved.

1. Introduction

Composite alloys made by reinforcing crystalline alloy with fiber particles have attractive physical and mechanical properties as compared to unreinforced alloys [1,2]. It was reported that the mixture of WC particles in NiSiB amorphous ribbons was effective for obtaining a good wettability against the matrix phase [3]. Recently, synthesis of a bulk $Zr_{55}Al_{10}Ni_{15}Cu_{30}$ amorphous matrix composite (AMC) with ZrC particles [4] and a ZrNbAlCuNi amorphous matrix with WC particles [5] has been reported. The composites were made by introducing directly ce-

ramics such as SiC, WC and ZrC particles into the amorphous alloy (a-alloy). The synthesis of the composite alloy consisting of crystalline particles in bulk amorphous matrix is a promising way to further improve mechanical properties of the bulk a-alloys and develop new bulk metastable materials. In this work, $Zr_{41}Ti_{14}Cu_{12.5}Ni_{10}Be_{22.5}$ bulk a-alloy, which exhibits best glass-forming ability (GFA) [6], was used as matrix; the interfacial reaction between carbon addition and the constituents in the molten glass forming alloy was used to prepare the bulk AMC. This method has the advantage of uniformly mixing the formed crystalline particles into the amorphous matrix, and offering isotropic properties with substantial improvements in strength. X-ray diffraction (XRD), optical microscopy, differential scanning

---

* Corresponding author.
  E-mail address: whw@aphy.iphy.ac.cn (W.H. Wang).

calorimetrically (DSC) and Vickers microhardness (HV) measurements are applied to study the structure, GFA, thermal and mechanical properties of the bulk AMC. The strengthening mechanism of the crystalline particles in amorphous matrix is discussed.

2. Experimental

To get $Zr_{41}Ti_{14}Cu_{12.5}Ni_{10}Be_{22.5}$ AMC, a Ni–C master alloy was first prepared by sintering the mixture of pure Ni powder (99.999%) and pure C powder (99.99%) in a vacuum (better than 10^{-5} Pa) to a solid lump. Because the solubility of C in Ni is only about 2.5 at.%, the lump is then the mixture of C and Ni. The solubility of carbon in other constituents of the alloy is also negligible [7]. Ti, Zr, Cu, Be elements and the NiC lump were inductive levitation melted together under a Ti-gettered Ar atmosphere with oxygen partial pressure of 10^{-9} Pa, and then quenched in a copper mold to form an ingot. The carbon is then uniformly mixed into the alloy. The sample was weighed at various stages of the alloying process to check the loss of the product. The weight loss after melting was less than 0.1%, the composition of the alloys did not change significantly after melting. Cross-sections of the ingot were investigated by XRD, DSC, scanning electron microscope (SEM), ultrasonic technique and microhardness. The structural nature was determined by XRD performed on a Siemens D5000 diffractometer with Cu K$_\alpha$ radiation. The thermal stability, glass transition and crystallization behaviors were studied by using DSC in a calibrated high-temperature Netzsch DSC 404 calorimeter under flowing pure Ar gas. Vickers hardness (HV) was obtained at a testing load of 1.96 N. SEM coupled with energy-dispersive X-ray spectroscopy was performed on Jeol JSM-U3, 20 kV acceleration voltage. The ultrasonic measurements were measured by using the pulse echo overlap method, the travel time of ultrasonic waves propagating through the sample with a 10-MHz carrying frequency which was measured using a MATEC 6600 ultrasonic system with a measuring sensitive of 0.5 ns.

3. Results and discussion

Fig. 1 shows XRD pattern for the $Zr_{41}Ti_{14}Cu_{12.5}Ni_{10}Be_{22.5}$ alloy with 4 at.% carbon addition. The pattern from the carbon powder and $Zr_{41}Ti_{14}Cu_{12.5}Ni_{10}Be_{22.5}$ a-alloy is also shown for comparison. The curve of the sample with carbon addition shows a superimposition of broad maximum from the amorphous phase and a number of sharp peaks characteristic of a crystalline phase, suggesting the presence of a mixture of the amorphous and crystalline phases. The position and the intensity of the crystalline peaks match exactly with that of ZrC carbide as shown in Fig. 1. No other phases are detected within the sensitivity limits of the XRD. The results indicate that 4% carbon addition induces the formation of bulk ZrTiCuNiBe AMC, consisting of ceramic fcc-ZrC particles. The fabrication of the
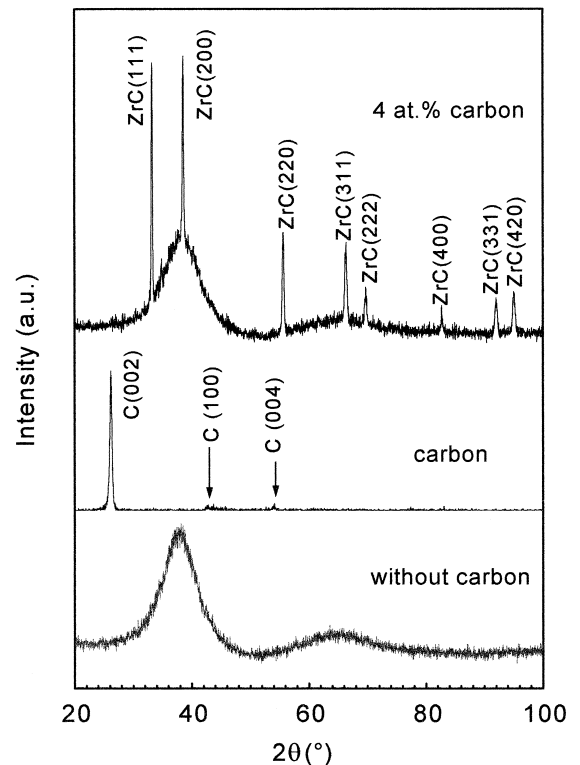

Fig. 1. The XRD patterns for the water-quenched ZrTiCuNiBe matrix. Composite alloy with 4 at.% carbon addition. The XRD curves of the $Zr_{41}Ti_{14}Cu_{12.5}Ni_{10}Be_{22.5}$ a-alloy and the pure alloy with the added carbon are also shown for comparison.

bulk AMC containing the homogeneously ZrC particles is up to 8 % carbon addition. Fig. 2 displays the optical micrograph of the composite. The crystalline particles embedded in the amorphous matrix are uniformly distributed. The average size and the volume fraction of the particles are about 9 μm and 8%, respectively. SEM with energy-dispersive X-ray analysis shows that the crystalline particles contain only carbon and Zr, confirming that the crystalline particles are ZrC carbide. Furthermore, neither pores nor voids are seen over the whole SEM micrograph, indicating that true bondy state exists at the interfaces between the amorphous matrix and ZrC particles. TEM results also confirm that there are no crystalline phase voids between the amorphous matrix and ZrC particles.

The crystalline ZrC carbide is formed from the interfacial reaction between carbon and molten Zr. It is known that C can form strong covalent bonds with the constituents in the alloy and cause the formation of crystalline compounds with high melting temperature [8]. On the other hand, the constituents have large negative heat of mixing and high reactivity with C [9]. These factors are the favorable factors for the solid–liquid reaction between C and the molten constituents [10]. It was found that even the structure of C_{60} can be disrupted by the solid state reaction between the transition metals and C and form carbide during low-temperature annealing [11]. Zr has a
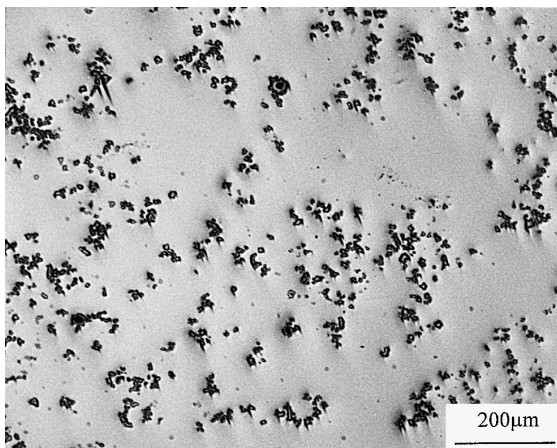

Fig. 2. An optical micrograph for the ZrTiCuNiBe matrix composite. The average size of the particle is about 9 μm. The volume fraction is about 8%.
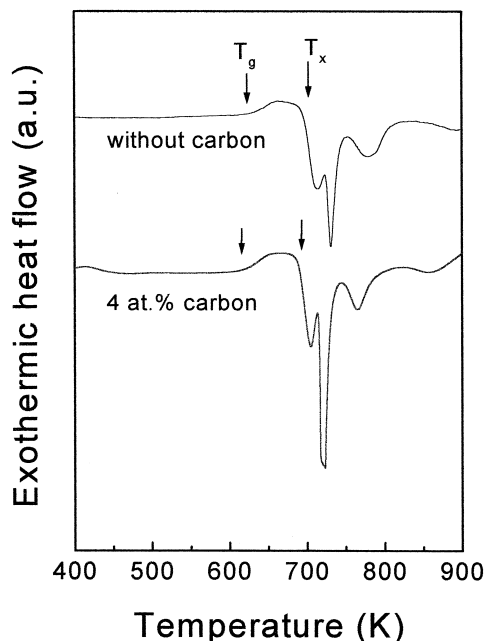

Fig. 3. DSC traces of the $Zr_{41}Ti_{14}Cu_{12.5}Ni_{10}Be_{22.5}$ amorphous matrix composite with 4% carbon addition and $Zr_{41}Ti_{14}Cu_{12.5}Ni_{10}Be_{22.5}$ a-alloy.

much larger negative heat of mixing (109 kJ/mol) [9] with C than that of other constituents, meaning that Zr and C have the largest driving force for the reaction. Thus, the C and Zr reaction is favored, and the reaction leads to a uniform dispersion of the ZrC particles.

A comparison of DSC traces measured at heating rate of 10 K/min for the $Zr_{41}Ti_{14}Cu_{12.5}Ni_{10}Be_{22.5}$ a-alloy and the bulk AMC is given in Fig. 3. Both alloys exhibit an endothermic heat event characteristic of the glass transition followed by three exothermic heat release events indicating the successive stepwise transformations from supercooled liquid state to crystalline phases. The peaks correspond to the formation of a Laves phase with hcp ''MgZn2-type'' structure, a phase with the ''Al_2Cu-type'' structure and one additional unidentified phase [12]. For the a-alloy, the glass transition temperature T_g, the onset temperature of the first crystallization event T_{x1}, and $\Delta T = T_{x1} - T_g$, referred as to the supercooled liquid region are 623, 683 and 60 K, respectively. There is no discernible difference between the two DSC curves. It is known that ΔT, which has

good correlation with the GFA, can represent the GFA of the bulk a-alloy [6,13,14]. So, the DSC result indicates that the GFA and the thermal stability of the amorphous matrix are not significant changed by 4% carbon addition. In fact, the reaction between C and the matrix changes the composition of the matrix, and removes the composition of the alloy out of the optimum glass-forming range. It seems that the carbon addition would lower the GFA and thermal stability of the amorphous matrix. The observed opposite results can be understood in two aspects. On one hand, the alloy has excellent GFA in quite wide glass-forming range [6], the small composition change does not significantly degrade its GFA and thermal stability. On the other hand, little dissolution of carbon (about 1 at.%) into the matrix can enlarge the thermal stability of the amorphous matrix [15]. The improved thermal stability of the matrix by dissolution of reinforcement has also been observed in Si addition in Cu–Ti–Zr–Ni a-alloy [16].

Fig. 4 shows the influence of carbon addition on the HV of the alloy. The HV increases with increasing carbon content; the HV of the composite with 4% carbon increases to 7.20 GPa, which is about 1.8 GPa larger than that of the $Zr_{41}Ti_{14}Cu_{12.5}Ni_{10}Be_{22.5}$ a-alloy (5.40 GPa). The elastic behavior studied by ultrasonic technique shows that the Young's modulus E changes from 90 GPa [6] for the homogenous $Zr_{41}Ti_{14}Cu_{12.5}Ni_{10}Be_{22.5}$ a-alloy to 106 GPa for the a-alloy with 1% carbon addition [17], indicating that little C addition can enhance the strength of the a-alloy. The uniformly dispersed ZrC particles induced by carbon and molten Zr interfacial reaction increase effectively the strength of the AMC.

The mechanical strengthening in the AMC obeys approximately the simple mixture rule that was commonly used to predict the properties of the metal matrix composites [16], since the E and HV of the ZrC carbide have been reported to be 390 and 32 GPa, respectively [18]. The similar tendency was also found for ZrAlNiCu AMC containing ZrC particle [4]. This result indicates that the strengthening mechanism of the dispersed carbide particles may be similar to that of metal matrix composites, which have been related to a high dislocation density in the matrix originating from differential thermal contraction, geometrical constraints during the processing [19]. The strengthening could be obtained by hindering propagation of the cracks and shear bands in the AMC due to the existence of the crystalline ZrC particles.

4. Conclusion

The fine precipitation of the fcc-ZrC crystalline carbide in the bulk a-alloy is formed by the reaction between added carbon and the molten glass-forming alloy. The bulk $Zr_{41}Ti_{14}Cu_{12.5}Ni_{10}Be_{22.5}$ AMC containing reaction-induced ceramic ZrC particles yields an improved microhardness in comparison to the a-alloy. The interfaces between the crystalline particles and amorphous matrix hinder the propagation of the microcracks formed under applied external stress in the AMC and result in the improvements of the mechanical property. The method for synthesizing the bulk AMC is effective and important for further development of bulk metastable materials.
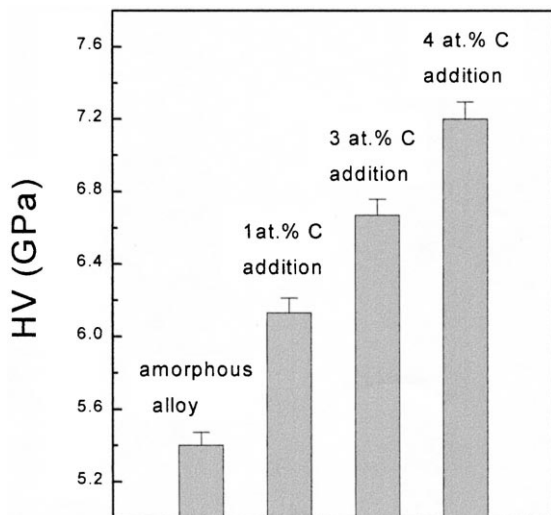

Fig. 4. A comparison of the Vickers hardness (HV) changes with increase of the carbon content in the $Zr_{41}Ti_{14}Cu_{12.5}Ni_{10}Be_{22.5}$ a-alloy.

References

[1] T. Christman, A. Needlman, S. Suresh, Acta Metall. 37 (1989) 3029.
[2] M.F. Ashby, F.J. Blunt, M. Bannister, Acta Metall. 37 (1989) 1847.
[3] H. Imura, T. Masumoto, D.G. Ast, Acta Metall. 35 (1987) 1757.
[4] H. Kato, A. Inoue, Mater. Trans. JIM 38 (1997) 793.
[5] H. Choi-Yim, W.L. Johnson, Appl. Phys. Lett. 71 (1997) 3808.
[6] W.L. Johnson, Mater. Sci. Forum 225–227 (1996) 35.
[7] Th.B. Massalski (Ed.), Binary Alloys Phase Diagrams, American Society for Metals, Metals Park, OH, 1986.
[8] B.M. Clemens, R. Sinclair, MRS Bull. 15 (1990) 19.
[9] F.R. De Boer, R. Boom, W.C.M. Mattens, A.R. Miedema, A.K. Niessen, Cohesion in Metals, North-Holland, Amsterdam, 1988.
[10] W.L. Johnson, Prog. Mater. Sci. 30 (1986) 81.
[11] W.H. Wang, W.K. Wang, J. Appl. Phys. 79 (1996) 149.
[12] C.J. Gilbert, R.O. Ritchic, W.L. Johnson, Appl. Phys. Lett. 71 (1997) 476.
[13] A. Inoue, Mater. Trans. JIM 36 (1995) 866.
[14] W.H. Wang, Q. Wei, S. Fridrich, Phys. Rev. B 57 (1998) 8211.
[15] W.H. Wang, Q. Wei, H.Y. Bai, Appl. Phys. Lett. 71 (1997) 58.
[16] I.A. Ibrahim, F.A. Mohamed, E.J. Lavernia, J. Mater. Sci. 26 (1991) 1137.
[17] W.H. Wang, R.J. Wang, F.Y. Li, D.Q. Zhao, M.X. Pan, Appl. Phys. Lett. 74 (1999) 1083.
[18] Metals Databook, Japan Inst. Metals, Maruzen, Tokyo, 1974, p. 141.
[19] R.J. Arsenault, R.M. Fisher, Scr. Metall. 17 (1983) 67.